Structure and Density of Mo and Acid Sites in Mo-Exchanged H-ZSM5 Catalysts for Nonoxidative Methane Conversion

Richard W. Borry III, Young Ho Kim, Anne Huffsmith, Jeffrey A. Reimer, and Enrique Iglesia*

Materials Sciences Division, E.O. Lawrence Berkeley National Laboratory, and Department of Chemical Engineering, University of California, Berkeley, California 94720

Received: March 12, 1999; In Final Form: May 7, 1999

Mo/H-ZSM5 (1.0−6.3 wt % Mo; Mo/Al = 0.11−0.68) catalysts for CH_4 aromatization were prepared from physical mixtures of MoO_3 and H-ZSM5 (Si/Al = 14.3). X-ray diffraction and elemental analysis of physical mixtures treated in air indicate that MoO_x species migrate onto the external ZSM5 surface at about 623 K. Between 773 and 973 K, MoO_x species migrate inside zeolite channels via surface and gas phase transport, exchange at acid sites, and react to form H_2O. The amount of H_2O evolved during exchange and the amount of residual OH groups detected by isotopic equilibration with D_2 showed that each Mo atom replaces one H^+ during exchange. This stoichiometry and the requirement for charge compensation suggest that exchanged species consist of $(Mo_2O_5)^{2+}$ ditetrahedral structures interacting with two cation exchange sites. The proposed mechanism may provide a general framework to describe the exchange of multivalent cations onto Al sites in zeolites. As the Mo concentration exceeds that required to form a MoO_x monolayer on the external zeolite surface (∼4 wt % Mo for the H-ZSM5 used), Mo species sublime as $(MoO_3)_n$ oligomers or extract Al from the zeolite framework to form inactive $Al_2(MoO_4)_3$ domains detectable by ^{27}Al NMR. These $(Mo_2O_5)^{2+}$ species reduce to form the active MoC_x species during the initial stages of CH_4 conversion reactions. Optimum CH_4 aromatization rates were obtained on catalysts with intermediate Mo contents (∼0.4 Mo/Al), because both MoC_x and acid sites are required to activate CH_4 and to convert the initial C_2H_4 products into C_{6+} aromatics favored by thermodynamics.

Introduction

The selective conversion of natural gas to higher hydrocarbons and aromatics remains an important industrial challenge. The discovery of catalytic CH_4 aromatization on Mo/H-ZSM5[1] was followed by several reports of near-equilibrium CH_4 conversions at 973 K with high selectivity to benzene. [2−4] CH_4 reaction rates increased with time on stream as dispersed MoO_x formed the active MoC_x species.[3] Ethylene and ethane are formed on MoC_x sites as primary products and they convert to C_{6+} aromatics via oligomerization, cracking, and cyclization reactions. These reactions require chain growth and dehydrogenation steps that occur on Bronsted acid sites aided by hydrogen desorption sites provided by MoC_x species. The net reaction rate is limited by the rate of CH_4 activation and by the approach to thermodynamic equilibrium of the overall methane aromatization reaction.[3]

In previous studies, Mo/H-ZSM5 catalysts were prepared by slurry or incipient wetness impregnation of H-ZSM5 with aqueous ammonium heptamolybdate (AHM; $(NH_4)_6Mo_7O_{24}$) solutions, followed by treatment in air at 723−973 K.[1−4] Large aqueous molybdate ions do not exchange directly onto H-ZSM5 cation exchange sites during impregnation.[5] Infrared spectroscopy and differential thermal analysis[6] showed that AHM decomposed in air between 500−650 K to form MoO_3 crystallites on the outer surface of zeolite crystals.[7,8] At 773 K, MoO_3 infrared bands disappeared as MoO_3 crystallites dispersed on the external surface of ZSM5 crystals and then migrated as $(MoO_3)_n$ oligomers into zeolite channels.[6] These authors concluded that MoO_x interacts with framework oxygens in H-ZSM5 at 973 K to form isolated monomolybdate species (MoO_4^{2-}) based on the appearance of infrared bands for Mo=O vibrations in tetrahedral Mo^{6+}.

Surface migration of MoO_x onto H-ZSM5 can occur at high temperatures because lattice mobility within MoO_3 becomes possible above its Tammann temperature (534 K).[9] Sublimation of MoO_3 becomes detectable above 623−673 K,[10] and MoO_3 reaches a vapor pressure of 56 Pa at 973 K[11] as $(MoO_3)_n$ oligomers ($n = 2-5$).[12] H_2O formed during decomposition of AHM precursors can form $MoO_2(OH)_2$,[12,13] which has a vapor pressure of 4.9 Pa at 973 K.[11]

As isolated MoO_x species migrate into zeolite channels via gas phase or surface diffusion, they react with H^+ atoms at exchange sites to form $(MoO_2(OH))^+$ species, which can condense with another one to form a $(Mo_2O_5)^{2+}$ dimer and H_2O:

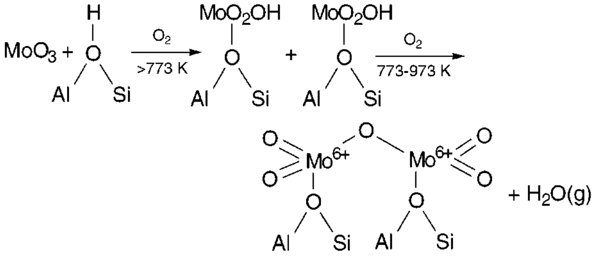

(1)

Throughout this report, we refer to these dimers as $(Mo_2O_5)^{2+}$ in spite of the fact that such cationic species are not known in

---

* Corresponding author. E-mail: iglesia@cchem.berkeley.edu.

10.1021/jp990866v CCC: $18.00 © 1999 American Chemical Society
Published on Web 06/25/1999

solution, because it is customary to think of exchanged species in zeolites as cationic. The stable structural analog is the known $(Mo_2O_7)^{2-}$ anion, consisting of two Mo centers with tetrahedral symmetry, with two of the oxygen atoms residing at framework positions in ZSM5. $(MoO_2(OH))^+$ species can also react with a zeolite OH group to form a $(MoO_2)^{2+}$ cation bridging two acid sites and water, a structure previously proposed for the exchange of MoO_2Cl_2 onto H-Y zeolite.[14]

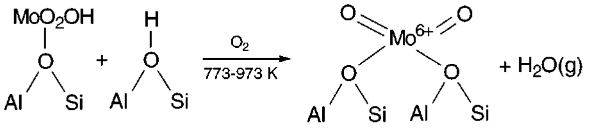

(2)

Similar condensation reactions of OH groups lead to the extraction of Al ions from the framework, with the formation of water and the disappearance of two Bronsted acid sites. In Mo/H-ZSM5, extraframework Al atoms form small domains of Al_2O_3 or $Al_2(MoO_4)_3$; the latter species were detected by ^{27}Al NMR in Mo/H-ZSM5 samples with high Mo content (>10 wt %).[15]

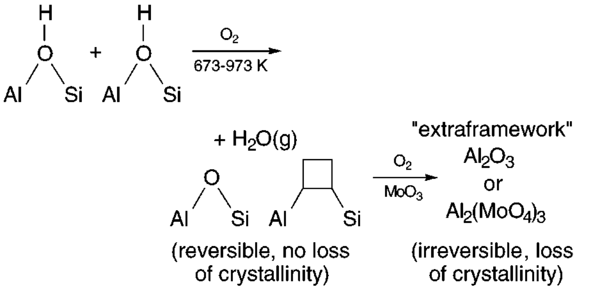

(3)

Impregnation or ion exchange of H-ZSM5 with AHM solutions leads initially to external MoO_3 crystals during treatment in air. Thus, it seemed possible to prepare Mo/H-ZSM5 via exchange from intimate mixtures of MoO_3 and H-ZSM5 powders. This approach avoids AHM decomposition products (N_2, NH_3, and H_2O)[6], which interfere with measurements of the kinetics and the extent of exchange from the amount of water evolved during synthesis. Here, we report mechanistic details of the synthesis of MoO_x/H-ZSM5 from mixtures of MoO_3 and H-ZSM5 powders, the structure of the MoO_x species formed during exchange, and the role and density of MoO_x species and of Bronsted acid sites in alkane reactions.

Experimental Section

Catalyst Synthesis and Characterization. H-ZSM5 was prepared by aqueous exchange (repeated four times) of Na-ZSM5 (Zeochem, Si:Al = 14.3) with 1.0 M NH_4NO_3 (Fisher) (~10 g Na-ZSM5/L). The samples were dried at 400 K for 24 h and treated in dry air at 773 K for 24 h (10−15 g of cat., 50 cm^3/min). Mo/H-ZSM5 was prepared from physical mixtures of MoO_3 (Johnson Matthey, 99.5% purity) and H-ZSM5; these mixtures were ground together for about 0.1 h in an alumina mortar and pestle. Powder X-ray diffraction patterns were obtained in a Siemens Diffractometer D5000 using Cu Kα radiation ($\lambda = 1.5406$ Å). Surface areas and pore volumes were obtained from N_2 physisorption at its boiling point (Autosorb 6; Quantachrome, Inc.), after treating samples at 773 K for 1 h in flowing dry air (Medical grade, Praxair).

The effect of air treatment was examined using MoO_3/H-ZSM5 mixtures (0.3 g, 0−8 wt % Mo) dried at 623 K for 24 h in 20% O_2/Ar (100 cm^3/min, Praxair, >99.999%). Samples were heated at 10 K/min to 973 K and H_2O evolution rates were measured by mass spectrometry (Leybold Inficon, THP-TS200) using heated transfer lines (373 K) and Ar as an internal standard. Samples were held at 973 K for 0.5 h and then cooled to 300 K. The number of residual OH groups in Mo/H-ZSM5 was measured from the evolution of HD and H_2 by mass spectrometry as samples were heated from 300 to 873 K (10 K/min, 2 min hold time) in 5% D_2/Ar (100 cm^3/min, Praxair, >99.999%).[16,17] Samples were then cooled to 300 K and the experiment was repeated using 5% H_2/Ar (100 cm^3/min, Praxair, >99.999%) while measuring HD and D_2 evolution rates. The Mo content was measured by atomic absorption (Galbraith Laboratories) after treatment in air at 973 K.

^{27}Al NMR spectra were collected using a home-built 400 MHz spectrometer (9.1 T magnetic field) at 104.2 MHz while spinning at 4 kHz.[18] Samples were hydrated at room temperature by placing them in an empty desiccator containing liquid water. Hydration of Al sites weakens quadrupole interactions that broaden ^{27}Al NMR lines in H-ZSM5.[19,20]

Steady-State CH_4 Aromatization on Mo/H-ZSM5. CH_4 reactions were carried out at 950 K in a tubular reactor (4 mm i.d.) with plug-flow hydrodynamics (25 cm^3/min, 1:1 CH_4/Ar (Praxair, >99.995%)). Mo/H-ZSM5 catalysts (1.0 g) were loaded onto a porous quartz disk (1.0 cm i.d.) located within this reactor. Temperatures were measured with a type K thermocouple located inside a quartz sheath in contact with the catalyst bed. The reactor effluent was sampled using transfer lines held at 400 K,[21] and the reactant and product concentrations were measured by gas chromatography.[22] Reported selectivities are defined as the percentage of the CH_4 converted appearing as a given product. CH_4 was used as the reference peak between the flame ionization and thermal conductivity detectors and Ar was used as an internal standard. The amount of carbon missing within the measured products (1−10%) is reported as “carbon” in the results, but it includes carbon consumed to form MoC_x and condensable products remaining in zeolite channels or in transfer lines. The reported values for CH_4 conversion, hydrocarbon yields, and carbon balances were reproducible within ±0.5% (absolute), and the detection limits were 50 and 1 ppm for thermal conductivity and flame ionization detectors, respectively. Catalysts were treated in 20% O_2/He (100 cm^3/min, Praxair, >99.999%) at 950 K for 2 h before catalytic reactions.[23]

Results

Catalytic CH_4 Aromatization on Mo/H-ZSM5. CH_4 reaction rates and selectivities measured on Mo/H-ZSM5 (4.0 wt %) prepared from MoO_3/H-ZSM5 mixtures (Figure 1) were similar to those reported on samples prepared by impregnation of H-ZSM5 with aqueous AHM (Table 1).[3] During the initial activation (~1−2 h), CH_4 conversion reached about 20%, but carbon, H_2, CO_2, H_2O, and CO were the most abundant initial products. After 2 h, CO and CO_2 were no longer detectable and the carbon selectivity was below 7%. Benzene (~70% selectivity), toluene (~5%), ethylene (4−8%), ethane (2−4%), and naphthalene (10−20%) were formed at CH_4 conversions of 7−10%. Propene and *o*-xylene were also detected in trace amounts (<2% selectivity). By comparison, a Mo/H-ZSM5 (2 wt %) sample prepared by impregnation of H-ZSM5 with aqueous AHM[3] gave 10% CH_4 conversion and 70% selectivity to benzene at 973 K (Table 1).

MoO_3 Migration and Sublimation during Catalyst Synthesis. Our initial measurements of the rate of MoO_x migration from the rate of H_2O evolution during treatment in air were influenced by MoO_3 sublimation from the physical mixtures. Heating MoO_3/H-ZSM5 mixtures (4.0 wt % Mo) from 300 to

TABLE 1: Comparison of CH_4 Aromatization on Mo/H-ZSM5 Prepared from Aqueous Impregnation of Molybdate Solution on H-ZSM5 and Physical Mixture of MoO_3/H-ZSM5

Mo content (wt %)	Mo/Al atomic ratio	reaction temp (K)	GHSV (h^{-1})	CH_4 conversion (%)	selectivity (%)			solid carbon
					C_2H_4	C_6H_6	$C_{10}H_8$	
2.0[a]	0.37	973	800	10.0	3	70	20	5
4.0[b]	0.42	950	750[d]	10.2	2	66	18	12
4.3[e]	0.45	950	750[d]	1.7	17	27	4	52

[a] Incipient wetness impregnation of AHM/H-ZSM5.[3] [b] Physical mixture of MoO_3/H-ZSM5 (this study). [c] "Vapor-exchanged" preparation method (this study, Figure 6). [d] Space velocity was calculated assuming catalyst packed density of 0.5 g cat./cm^3 reactor volume.

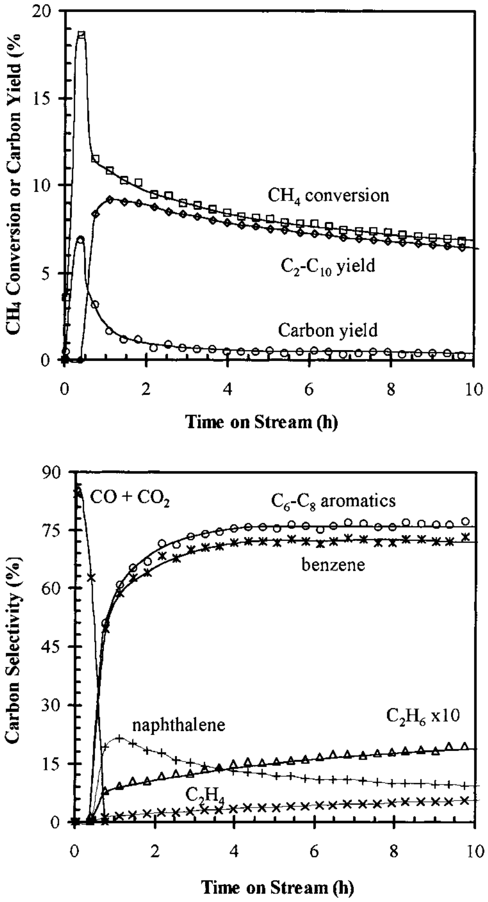

Figure 1. CH_4 pyrolysis on 4 wt % Mo/H-ZSM5, (a, top) CH_4 conversion, C_2-C_{10} hydrocarbon product yield, and solid carbon yield vs. time on stream, (b, bottom) carbon selectivity of gas-phase products vs time on stream (1.0 g, 25 cm^3/min, 50% CH_4/Ar, 105 kPa, 950 K).

TABLE 2: Mo Content after Temperature-Programmed Oxidation of MoO_3/H-ZSM5 Mixtures (∼4 wt % Mo, 0.3−1.0 g, 100 cm^3/min, 20% O_2 in He)

	temperature program	Mo as prepared[a] (wt %)	Mo after TPO[b] (wt %)
I	300 to 973 K (10 K/min)	4.0	3.47
II	300 to 623 K (hold 24 h) 623 to 973 K (10 K/min)	4.0	3.60
III	300 to 623 K (hold 24 h) 623 to 773 K (10 K/min, 48 h) 773 to 950 K (10 K/min, 2h)	3.94	3.95

[a] Based on amount of Mo added to physical mixture. [b] Based on elemental analysis of oxidized sample.

973 K (at 10 K/min) led to the sublimation of 13% of the Mo as $(MoO_3)_n$ or $MoO_2(OH)_2$ (Table 2, program I). The sublimed MoO_x appeared as small MoO_3 crystallites on the walls after the heated sample. When MoO_3/H-ZSM5 mixtures were held at 623 K for 24 h in order to remove physisorbed H_2O and to disperse MoO_x species onto the external zeolite surface, subsequent heating in air to 973 K led to Mo losses of less than 10% (Table 2, program II). The H_2O evolved during exchange appeared as a well-defined peak between 623 and 973 K (as shown later in Figure 3). Holding at 773 K for 48 h during treatment in air (Table 2, program III) eliminated Mo loss (<0.1%), apparently because MoO_x crystallites spread as strongly interacting layers with much lower vapor pressure than bulk MoO_3. This method was used to prepare the Mo/H-ZSM5 samples used in the reaction studies (Figure 1, Table 1).

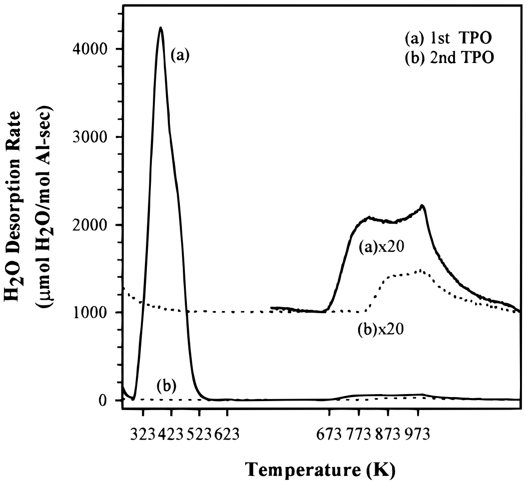

Figure 2. H_2O desorption from H-ZSM5 during first (a) and second (b) TPO. The sample was heated at 10 K/min from 323 to 623 K, held for 24 h, then heated at 10 K/min to 973 K (0.3 g, 100 cm^3/min, 20% O_2/Ar, 101 kPa).

H_2O Desorption during Oxidative Treatment of MoO_3/H-ZSM5 Mixtures. Figure 2 shows the H_2O evolution rate during temperature-programmed oxidation (TPO) of H-ZSM5 (using program II in Table 2). The peak at 300−500 K corresponds to the desorption of water adsorbed on H-ZSM5 from ambient air (2.62 mol H_2O/Al). The smaller peak between 673 and 973 K corresponds to zeolite dealumination (eq 3) by loss of OH groups and extraction of Al atoms from tetrahedral framework positions. A previous thermogravimetric study of H-ZSM5 reached similar conclusions.[24] Figure 2b shows H_2O evolution rates during a second TPO after cooling the sample in dry 20% O_2/Ar (100 cm^3/min) to room temperature. The physisorbed water peak is no longer detected and the dealumination peak was smaller and it appeared at higher temperature, indicating that the zeolite structure was stabilized against further dealumination by the initial treatment. The number of OH groups desorbed as H_2O during the first and second treatments corresponds to 0.23 and 0.06 H/Al, respectively.

H_2O evolution during TPO of a MoO_3/H-ZSM5 physical mixture (4.5 wt % Mo)[25] shows that the amount of physisorbed H_2O is slightly smaller than on H-ZSM5 (1.80 mol H_2O/Al), but the second peak is much larger (Figure 3). This reflects the anchoring of Mo at cation exchange sites to form Mo species containing OH groups and the subsequent condensation of these

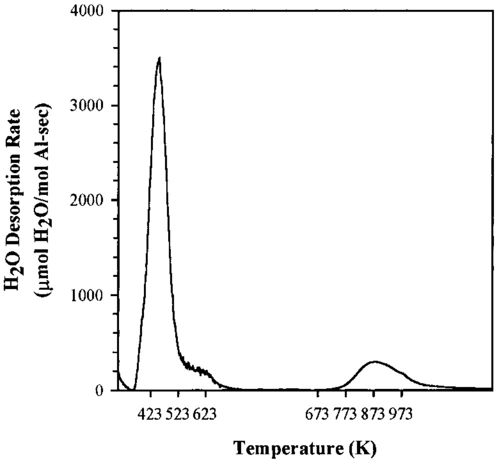

Figure 3. H_2O desorption from MoO_3/H-ZSM5 mixture (4 wt % Mo) during TPO. The sample was heated at 10 K/min from 323 to 623 K, held for 24 h, then heated at 10 K/min to 973 K (0.3 g, 100 cm^3/min, 20% O_2/Ar, 101 kPa).

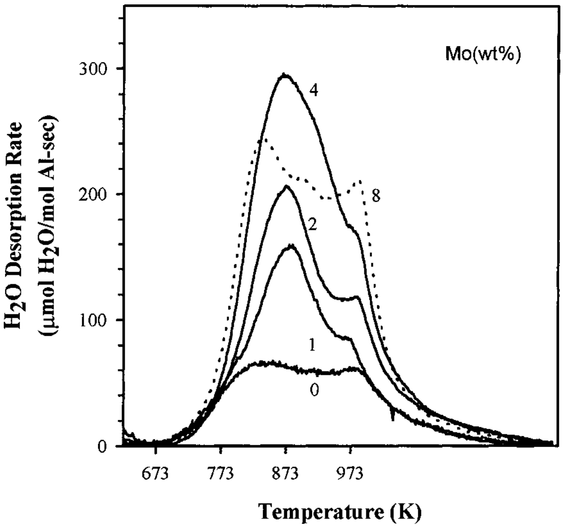

Figure 4. H_2O desorption between 623 and 973 K from MoO_3/H-ZSM5 mixtures with varying Mo initial concentration (0.3 g, 100 cm^3/min, 20% O_2/Ar, 101 kPa, heat at 10 K/min).

OH groups with those in H-ZSM5 or in neighboring Mo cations (eqs 1 or 2). The small difference in H_2O desorption rates below 623 K between H-ZSM5 (Figure 2) and MoO_3/H-ZSM5 mixtures (Figure 3) is caused by OH groups bound to MoO_3, and not by Mo exchange. This conclusion is confirmed by the observation that H_2O evolution rates between 623 and 773 K did not depend on Mo loading (Figures 4 and 14), suggesting that Mo cations migrate into channels and exchange only above 773 K, as also proposed by others.[26] Figure 4 shows that the amount of H_2O formed between 773 and 973 K increased with increasing Mo content. Some Mo sublimes from mixtures with more than 2 wt % Mo (Table 3) when treated by program II (Table 2); this was confirmed by elemental analyses before and after air treatment and by the MoO_3 residue formed at the exit of the treatment cell.

TABLE 3: Mo Content Measured by Atomic Absorption Spectrometry before and after Oxidation of MoO_3/H-ZSM5 Physical Mixtures of Varying Mo Concentration (Temperature Program II in Table 2, 0.3 g, 100 cm^3/min, 20% O_2 in He)

target Mo content (wt %)	analyzed Mo content in physical mixture (wt %)	Mo/Al before TPO	analyzed Mo content after TPO (wt %)	Mo/Al after TPO
1	1.1	0.11	1.0	0.11
2	2.2	0.22	2.0	0.20
4	4.0	0.42	3.6	0.37
8	7.9	0.87	6.3	0.68

TABLE 4: H_2O Desorption (TPO Program II, 0.3 g, 100 cm^3/min, 20% O_2 in He) and Isotopic Exchange (10 K/min, 100 cm^3/min, 5% (D_2 or H_2) in Ar) of MoO_3/H-ZSM5 Mixtures

Mo content after TPO (wt %)	Mo/Al ratio	H_2O desorption			residual H content		H balance[f] H/Al
		H/Al[a]	H/Al_F[b]	H/Mo[c]	H/Al[d]	D/Al[e]	
0	0	0.229	0		0.630	0.564	0.919[g]
1.0	0.11	0.347	0.118	1.11	0.400	0.456	0.803
2.0	0.20	0.474	0.245	1.22	0.254	0.355	0.829
3.6	0.37	0.686	0.457	1.23	0.099	0.170	0.856
6.3	0.68	0.665	0.436	0.64	0.035	0.107	0.772
4.3	0.45				0.019	0.074	

[a] From integrated area of H_2O desorption above 623 K (Figure 4). [b] Subtract value in column 3 from that for H-ZSM5 (0 wt % Mo). [c] Divide column 4 by Mo/Al ratio. [d] From $D_2(g)/O(s)-H$ isotopic exchange (Figure 9). [e] From $H_2(g)/O(s)-D$ isotopic exchange (Figure 10). [f] Sum of columns 3 and 7. [g] Includes second TPO and $D_2(g)/O(s)-H$ values (see text).

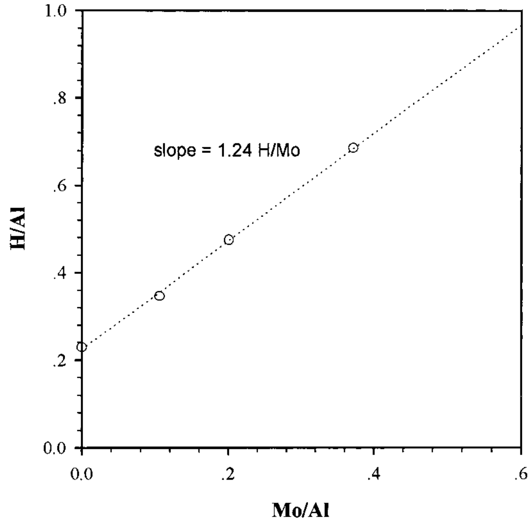

Figure 5. Number of H desorbed as H_2O per Al atom during treatment of MoO_3/H-ZSM5 mixtures in air to 973 K.

The number of H_2O molecules (per Al) formed during air treatment is shown in Table 4. If the loss of OH groups via recombination and Al extraction from framework positions occurred to the same extent in Mo/H-ZSM5 and H-ZSM5 samples, H_2O desorption values on Mo/H-ZSM5 can be corrected by subtracting the amount of H_2O desorbed from pure H-ZSM5 (0.23 H/Al, Table 4). These corrected values are reported as H/Al_F (Al_F = framework aluminum). This assumption was confirmed using ^{27}Al NMR to measure the change in intensity of the peak corresponding to tetrahedral (framework) Al centers (as discussed later). These data show that for samples with less than 4 wt % Mo, MoO_x species exchange with H^+ with a stoichiometry of about one Mo per H (Figure 5, slope = 1.24 H/Mo). For H-ZSM5 with a Si/Al ratio of 14.3, the number of cation exchange sites is not sufficient to accommodate all Mo atoms in the 8 wt % Mo sample, and the excess MoO_x sublimes above 773 K during air treatment.

Vapor-Exchange Synthesis from Separated MoO_3 and H-ZSM5 Powders. In a separate experiment, Mo/H-ZSM5 samples were prepared by flowing 20% O_2/He (100 cm^3/min) over bulk MoO_3 (0.185 g), and contacting the $(MoO_3)_n$ vapor with a bed of H-ZSM5 (1.509 g; Figure 6). The Mo content would be 7.3 wt % if all the MoO_3 remained in the exchanged

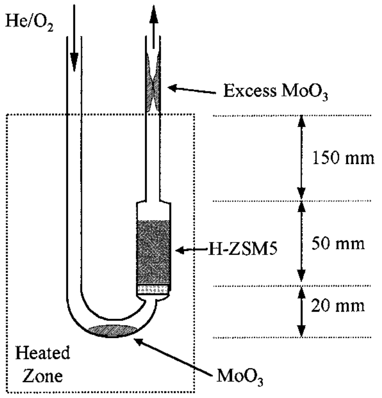

Figure 6. Preparation of "vapor-exchanged" Mo/H-ZSM5 sample (1.5 g, 50 cm^3/min, 20% O_2/He, 101 kPa, 950 K, 96 h).

TABLE 5: N_2 Physisorption at 77 K of MoO_3/H-ZSM5 Mixtures after TPO and TPR Treatment in Air and H_2 (D_2) to 973 K

Mo concn (wt %)	BET surface area (m^2/g zeolite)	micropore volume (cm^3/g zeolite)
0	272	0.128
1.1	278	0.119
2.0	266	0.120
3.6	218	0.107
6.3	132	0.059
4.3[a]	201	0.084

[a] Prepared via MoO_3 vapor exchange at 950 K, 96 h (see text).

samples after treatment in air. All the MoO_3 powder sublimed after 96 h at 950 K, contacted the H-ZSM5 sample, and either exchanged at ZSM5 sites or deposited as light green crystals (bulk MoO_3) on colder reactor walls above the zeolite bed. The resulting Mo/H-ZSM5 contained 4.3 wt % Mo. These results showed that surface diffusion is not required for MoO_x migration during treatment in air at high temperature (>873 K) and that vapor-phase transport of $(MoO_3)_n$ oligomers can occur during synthesis of Mo/H-ZSM5 from physical mixtures. CH_4 aromatization reaction rates were very low on this sample. At a space velocity of 750 h^{-1}, CH_4 conversion was only 1.7% (cf. 4.3 wt % Mo sample; Table 1).

Zeolite Structural Changes during Thermal Treatment of MoO_3/H-ZSM5 Mixtures. The unusual shape of the H_2O evolution rates on the 8 wt % Mo/H-ZSM5[27] (Figure 4) suggested some structural differences between this sample and the others, which we explored using powder X-ray diffraction (XRD), N_2 physisorption, and ^{27}Al NMR. N_2 physisorption results were used to estimate surface areas and micropore volumes (Table 5). Neither diffraction nor N_2 physisorption data showed any structural degradation of the zeolite in samples with 1.0 or 2.0 wt % Mo relative to pure H-ZSM5, but both methods detected a modest loss of crystallinity in the 3.6 and 4.3 wt % Mo samples, and significant destruction of the zeolite framework in the 6.3 wt % sample.[27] A loss of surface area with increasing Mo content was previously reported also for MoO_x/ZSM5 prepared by AHM slurry methods.[28]

^{27}Al NMR spectroscopy can probe the local structure of Al cations in Mo/H-ZSM5 samples. Tetrahedral Al centers in the zeolite framework bonded to terminal O−H groups have a chemical shift of 56 ppm; extraframework octahedral Al centers (in ZSM5 and in Al_2O_3) show no shift ($\delta = 0$ ppm), while crystalline $Al_2(MoO_4)_3$ (octahedral Al, tetrahedral Mo) shows a line at −13 ppm.[15] ^{27}Al NMR spectra for MoO_x/H-ZSM5 samples (Figure 7) showed that the density of unperturbed framework Al centers (corresponding to Bronsted acid sites) decreased with increasing Mo content. ^{27}Al NMR lines corresponding to crystalline $Al_2(MoO_4)_3$ appeared in the 6.3 wt % Mo/H-ZSM5 sample.[27] The $Al_2(MoO_4)_3$ crystallites are too small to be detected by X-ray diffraction in this sample, but they become detectable in Mo/H-ZSM5 samples with higher Mo content (15 wt %).[15]

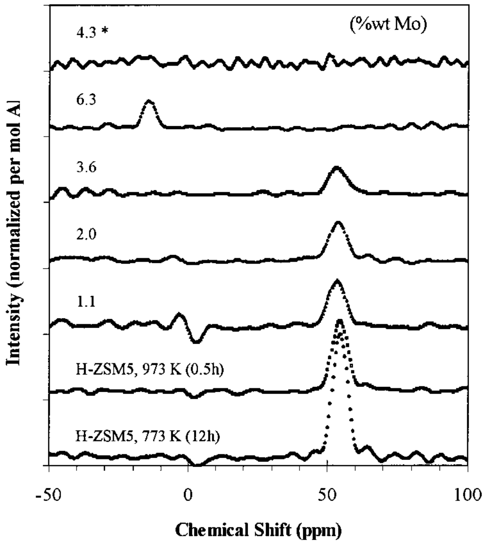

Figure 7. ^{27}Al NMR spectra of MoO_3/H-ZSM5 physical mixtures after TPO and TPR treatments to 973 K (*) 4.3 wt % Mo sample prepared via MoO_3 vapor exchange at 950 K, 96 h.

Thus, it appears that the unusual shape of the H_2O desorption curve for 6.3 wt % Mo/H-ZSM5 reflects the extraction of Al from the framework to form $Al_2(MoO_4)_3$ and the concomitant collapse of the zeolite pore structure. H_2O desorption rates from mixtures initially containing 4 and 8 wt % Mo were identical up to about 850 K (Figure 4), indicating that MoO_x-induced extraction of framework Al did not occur below 850 K. This agrees with ^{27}Al NMR data for 15 wt % Mo/H-ZSM5, which showed $Al_2(MoO_4)_3$ in samples treated in air at 873 or 973 K, but not in those treated at 773 K.[15] The ratio of OH groups removed as H_2O to Mo atoms in the 6.3 wt % Mo sample is only 0.64; this value is very similar to that expected for $Al_2(MoO_4)_3$ (0.67), but it is smaller than in Mo/H-ZSM5 samples with lower Mo content.

Isotopic Equilibration of D_2 with OH Groups in Mo/H-ZSM5 Samples. The isotopic equilibration of surface O−H groups with D_2 was carried out after treating Mo/H-ZSM5 in air at 973 K (procedure II, Table 2). This method was used previously in order to determine the number of OH groups in H-ZSM5 and cation-exchanged H-ZSM5.[16]

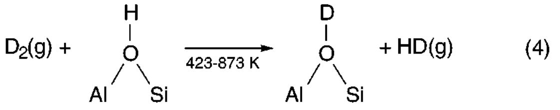

$$D_2(g) + \underset{Al\quad Si}{\overset{H}{O}} \xrightarrow{423\text{-}873\ K} \underset{Al\quad Si}{\overset{D}{O}} + HD(g) \qquad (4)$$

D_2/O−H exchange data are shown in Figure 8 for 3.6 wt % Mo/H-ZSM5 (prepared by program II; Table 2). The total number of H atoms removed as HD and H_2 corresponds to 0.1 H per Al. Figure 9 shows HD desorption rates during D_2/O−H exchange for all samples (0−6.3 wt % Mo; prepared by exchange in air at 973 K for 0.5 h). The number of O−H groups decreased with increasing Mo content, as O−H groups were increasingly replaced by Mo during exchange (eq 1). The data in Figure 9 also show that Mo species catalyze D_2 dissociation, the rate-determining step in D_2/O−H exchange, and thus

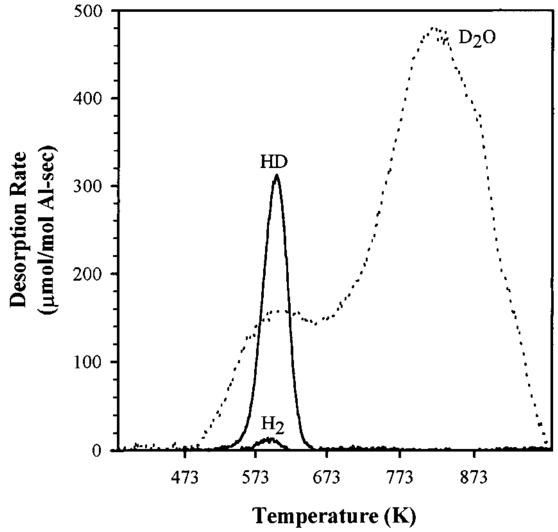

Figure 8. Production rate of H_2, HD, and D_2O during temperature-programmed $D_2(g)/O-H(s)$ isotopic exchange on 3.6 wt % Mo/H-ZSM5 (0.3 g, 100 cm^3/min 5% D_2/Ar, 101 kPa).

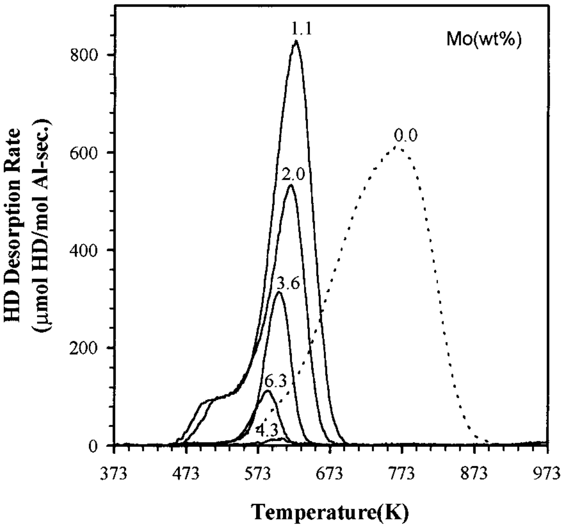

Figure 9. Rate of HD desorption during $D_2(g)/O-H(s)$ isotopic exchange on Mo/H-ZSM5 (0.3 g, 100 cm^3/min 5% D_2/Ar, 101 kPa).

decrease the temperature required for D_2-OH exchange by about 200 K.

The formation of D_2O during $D_2/O-H$ exchange above 500 K (Figure 8) reflects some reduction of Mo^{6+} species. This process influences the calculated exchange values, because both H_2O and HDO form via D_2O exchange with OH groups. H_2O and HDO contain H atoms from surface O−H groups, but their concentrations and isotopic contents are difficult to measure because of water adsorption and exchange on the heated walls of the cell and the transfer lines. These effects were shown to be small by cooling the samples to 300 K after $D_2(g)/O(s)-H$ exchange, and then heating to 973 K in flowing H_2; the measured amounts of HD and D_2 formed (Figure 10, denoted as $H_2(g)/O(s)-D$ exchange) gave densities of residual OD groups that were only slightly different from those measured from the initial D_2-OH exchange.

$D_2/O-H$ and $H_2/O-D$ exchange data show that each Mo added to H-ZSM5 replaces 1.0 ± 0.2 OH groups during exchange from physical mixtures at 973 K (Figure 11).[29] Tetrahedral Al atoms containing an OH group (Al_F) give a ^{27}Al NMR line that decreases in intensity as Mo content increases. These data allow us to calculate the fraction of the Al centers that interact with MoO_x species instead of OH groups (Figure 7), using a value of 0.92 for the Al_F/Al ratio in a H-ZSM5 sample pretreated in air at 773 K for 1 h (Table 4).[30] The results from D_2-OH, H_2-OD, and ^{27}Al NMR are in excellent agreement (Figure 11); they show that each Mo replaces one OH group, as expected for $(Mo_2O_5)^{2+}$ dimers bridging two cation exchange sites.

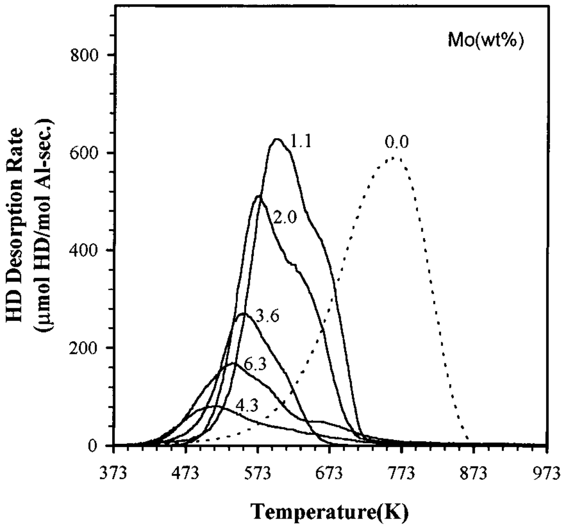

Figure 10. Rate of HD desorption during $H_2(g)/O-D(s)$ isotopic exchange on Mo/H-ZSM5 (0.3 g, 100 cm^3/min 5% D_2/Ar, 101 kPa).

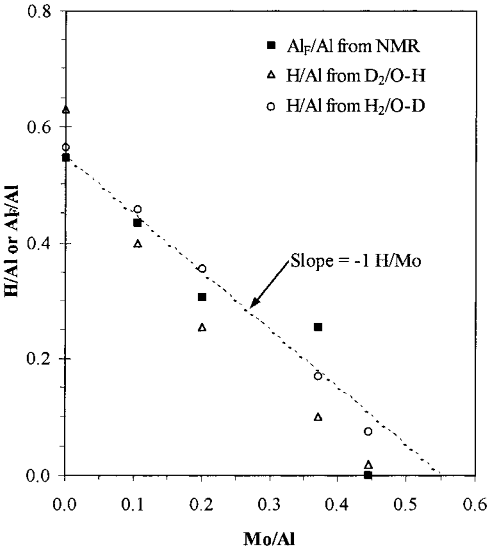

Figure 11. Number of acid sites (H) or framework Al (Al_F) remaining per total Al for series of Mo/H-ZSM5 samples after TPO and TPR treatment to 973 K (0.5 h) measured by ^{27}Al NMR, $D_2/O-H$, and $H_2/O-D$ (0.45 Mo/Al sample prepared via MoO_3 vapor exchange at 950 K, 96 h).

The sum of the OH groups removed as H_2O during exchange and those remaining (from $D_2/O-H$ data) should correspond to the total number of OH groups in the starting H-ZSM5 samples (Table 4). On H-ZSM5, the two TPO experiments and the D_2-OH exchange add to a value of 0.92 OH/Al (Table 4).[30] All Mo samples had values of 0.77−0.86 total OH/Al, in reasonable agreement with the value of 0.92 measured on H-ZSM5 (Table 4).

Discussion

X-ray diffraction, N_2 physisorption, and ^{27}Al NMR methods show that after treatment in air at 973 K, MoO_x/H-ZSM5

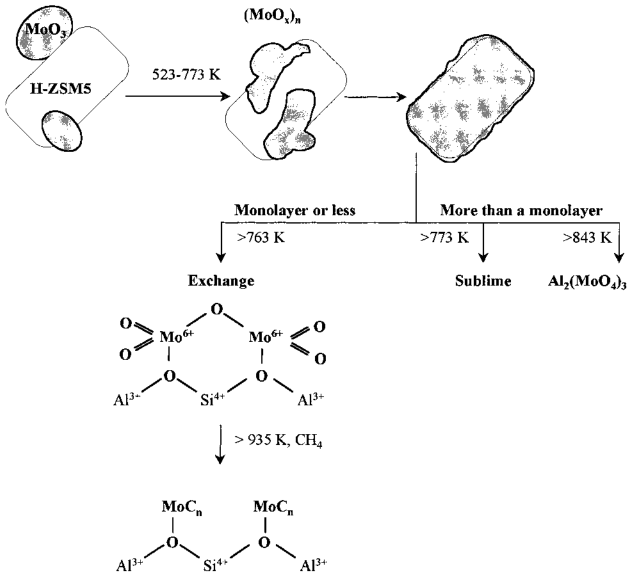

Figure 12. Formation of Mo/H-ZSM5 active sites from MoO_3/H-ZSM5 physical mixtures.

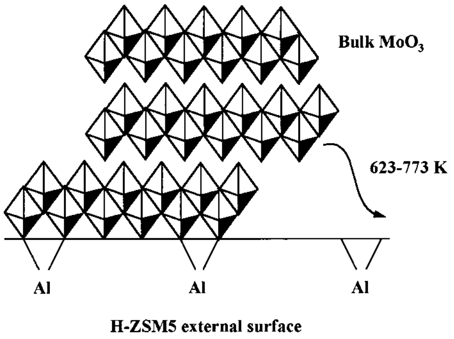

Figure 13. Structure of bulk MoO_3 and solid-state migration on H-ZSM5 surface.

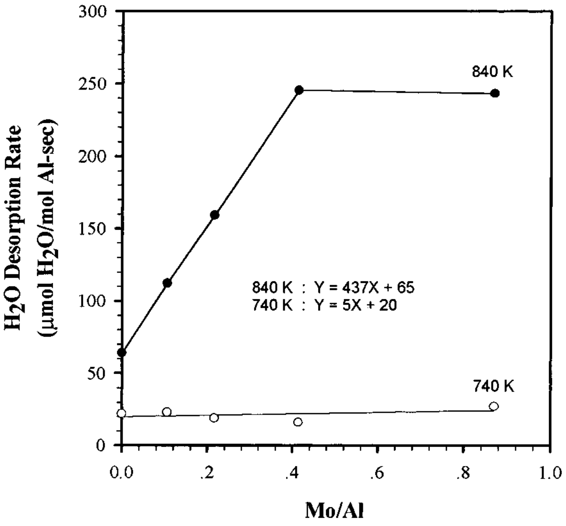

Figure 14. H_2O desorption rate during TPO of MoO_3/H-ZSM5 mixtures at 740 and 840 K (from Figure 4). (*) Mo/Al ratios are as prepared. Mo concentrations after TPO are shown in Table 3.

samples prepared from MoO_3−H-ZSM5 physical mixtures lead to exchanged Mo species similar to those obtained from aqueous exchange methods. Low pH conditions may alter the density and nature of external OH groups on zeolite crystals,[31] which can lead to MoO_x binding and may account for the high external Mo concentrations detected by X-ray photoelectron spectroscopy on samples prepared by aqueous exchange.[26,31] Methane conversion rates and selectivities are similar on samples prepared by the two methods, suggesting that active site densities and aromatization pathways are similar in MoO_x/H-ZSM5 samples prepared from physical mixtures (this study) and in those prepared using aqueous exchange.[1,3,6,28,32,33]

Migration of MoO_x Species during Treatment in Air. Our results are consistent with the processes depicted schematically in Figure 12. Below 623 K, X-ray diffraction shows that MoO_3 and H-ZSM5 crystallites remain intact. Between 623 K and 773 K, MoO_3 crystallites disappear as MoO_x migrates onto external zeolite surfaces. Knözinger, et al.[34] have proposed that MoO_3 spreads on Al_2O_3 surfaces via an "unrolling carpet" mechanism. Above 600 K, MoO_3 layers migrate until they reach AlO_x sites, where they anchor and become immobile (Figure 13). This process decreases surface energies as MoO_3 forms strong bonds with Al_2O_3; similar processes were not detected on SiO_2.[35] These data and the stability of $Al_2(MoO_4)_3$ suggest that Al−O−Mo bonds are stronger than Si−O−Mo bonds.[36]

MoO_3 consists of MoO_6 octahedra with displaced central Mo atoms.[37] MoO_6 octahedra form bilayers with van der Waals interlayer binding (Figure 13). Between 623 and 773 K, vibrations overcome this binding and bilayers slide over each other until they anchor at Al sites on external ZSM5 surfaces.[38] MoO_x species may also migrate into zeolite channels at these temperatures, but they do not react with O−H groups, as shown by the low rate of H_2O formation below ~750 K and by the lack of dependence of this rate on the Mo content (Figure 14).

After the external ZSM5 surface is covered completely with a MoO_3 layer above 773 K, further spreading cannot decrease the surface energy. In our study, samples with more than 4 wt % Mo contain more Mo than that required to form a MoO_3 monolayer on the external surface area of the ZSM5 crystals used. The excess MoO_x can sublime as $(MoO_3)_n$, as expected from the MoO_3 vapor pressure and from the observed loss of Mo in samples with high Mo content (Table 3). Excess Mo can also migrate into ZSM5 channels as isolated MoO_x species (as shown by the disappearance of XRD peaks and by the observed increase of H_2O desorption rate above 773 K; Figure 14) or extract Al from the ZSM5 framework to form $Al_2(MoO_4)_3$ (detected in the 8 wt % Mo sample by ^{27}Al NMR and confirmed by the unusual shape of the H_2O desorption curve for this sample above 850 K; Figure 4).

The strong Al−O−Mo interactions that lead to the spreading of MoO_3 on external zeolite surfaces also prevent MoO_3 sublimation. Thus, physical mixtures with less Mo than that required to form a single MoO_3 layer (1−2 wt % Mo) do not lose Mo by sublimation. The mixture containing 4 wt % Mo required treatment in air at 773 K for 24 h in order to attain full spreading of a MoO_x layer and to avoid sublimation during exchange (Table 2, program III). Even after this treatment, the 8 wt % Mo/H-ZSM5 sample lost about 20% of its MoO_3 by sublimation (Table 3). This shows that the maximum MoO_3 coverage for the external (mesoporous) surface area of the ZSM5 used (24 m^2/g) corresponds to about 4 wt % Mo.[39]

H_2O evolution rates (per Al or g-catalyst) during air treatment of MoO_3/H-ZSM5 mixtures at high temperatures (Figure 4) reflect the rate of replacement of H^+ with cationic Mo oxo species. This rate of exchange in turn depends on the mobility of migrating Mo species and on the number of ZSM5 channels available for transport. Below 740 K, H_2O evolution rates are independent of Mo content (Figure 14), indicating that MoO_x species do not undergo the condensation reactions that anchor them at exchange sites. Between 750 and 850 K, H_2O evolution rates become proportional to the Mo content for samples with

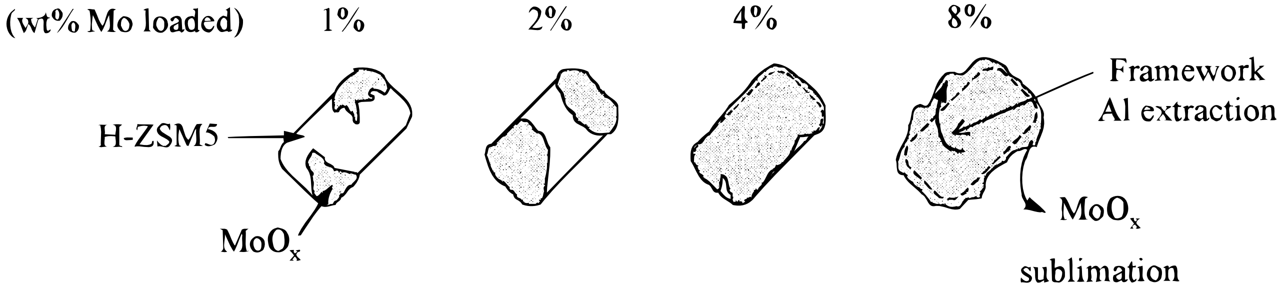

(5)

1.0−3.6 wt % Mo (Mo/Al = 0.11−0.37; Figure 14). These data suggest that zeolite channels become accessible to the external MoO_3 surface layer in proportion to the amount of Mo spread as a layer on the external zeolite surface (at least up to 3.6 wt % Mo). At higher Mo contents, H_2O desorption rates remain constant as temperatures increase from 750 and 850 K, suggesting that the external MoO_3 exceeds one monolayer and that all channel openings become accessible to MoO_3; then, condensation reactions become limited by rate of Mo migration within ZSM5 channels. These data are consistent with the scheme in eq 5 and with expected formation of a single MoO_3 layer in the 3.6 wt % Mo samples for the external area available in the H-ZSM5 crystals used in the physical mixtures.

On the sample with the highest Mo content (7.9 wt % Mo in mixture; 6.3 wt % after exchange), multiple MoO_3 layers can form on external zeolite surfaces. Above 843 K, AlO_x species can be extracted from the aluminosilicate and dissolved into liquidlike MoO_3 layers, within which they can react to form stable $Al_2(MoO_4)_3$ domains. $Al_2(MoO_4)_3$ was detected by ^{27}Al NMR and X-ray diffraction[15] in samples with high Mo content. In our study, $Al_2(MoO_4)_3$ was not detected in samples with less than 4 wt % Mo, because MoO_3 monolayers apparently lack the local three-dimensional structure and the thermodynamic incentive required to stabilize Al in $Al_2(MoO_4)_3$ structures.

The extraction of AlO_x species from the aluminosilicate framework to form $Al_2(MoO_4)_3$ causes the structural collapse detected by X-ray diffraction and N_2 physisorption measurements in the Mo/H-ZSM5 sample with 6.3 wt % Mo.[27] High temperatures alone do not cause the observed structural collapse, because "vapor-exchanged" (4.3 wt % Mo) samples were treated at 950 K for 96 h without significant loss of crystallinity and ^{27}Al NMR did not detect any $Al_2(MoO_4)_3$. It appears that high local MoO_x concentrations are required in order to extract Al from the aluminosilicate framework. The sample with 6.3 wt % Mo (7.9 wt % Mo in starting mixture) and the vapor-exchanged sample were exposed to similar MoO_x concentrations (7.9 wt % vs 7.3 wt % Mo), but vapor-exchanged samples were contacted by $(MoO_3)_n$ ($n \sim 3-4$) oligomers at a pressure of about 25 Pa (250 ppm),[11] while the 8 wt % Mo sample contained significant interfacial area between liquidlike bulk MoO_3 and zeolite surfaces. Thus, local MoO_3 concentrations are lower during vapor exchange synthesis (Figure 6), because $(MoO_3)_n$ oligomers adsorb onto the ZSM5 surface, migrate within zeolite channels, and bind irreversibly at sites where they form Mo−O−Al bonds before high local MoO_3 concentrations are reached.

Exchange of Cationic Mo Oxo Species via Condensation Reactions. The amount of water evolved during exchange and the number of O−H groups remaining after exchange show that each migrating MoO_x replaces one H^+ in H-ZSM5 (Figures 5 and 11). These data and the required charge balance suggest that $(Mo_2O_5)^{2+}$ dimers interacting with two exchange sites form during exchange (eq 1), which acquire the ditetrahedral structure of $(Mo_2O_7)^{2-}$ dimers when two framework oxygen atoms provide the anchoring sites for such dimers. Infrared bands corresponding to tetrahedral Mo^{6+} centers were detected previously but incorrectly assigned to $(MoO_4)^{2-}$ monomers bridging two exchange sites,[6] a stoichiometry that is not consistent with our results. The size of $(Mo_2O_7)^{2-}$ ditetrahedra in tetra-*n*-butylammonium dimolybdate (~5.7 Å)[40] and simple geometrical considerations based on a ZSM5 crystal structure with randomly distributed Al ions showed that about 60% of the Al atoms in H-ZSM5 (Si/Al = 14) can reside sufficiently close to another Al to allow Mo dimers to bridge Al pairs.[41] The exclusive presence of $(Mo_2O_5)^{2+}$ dimers is then possible at all Mo/Al ratios below 0.6 (i.e., <5 wt % Mo for our Si/Al zeolite ratio).

^{27}Al NMR shows that all Al centers in vapor-exchanged Mo/H-ZSM5 have been displaced from framework crystallographic positions (Figure 7). Thus, either Al centers are interacting with $(Mo_2O_5)^{2+}$ dimers or they have been extracted from the framework via condensation of two O−H groups at next nearest neighbor Al atoms. All Al−OH species in H-ZSM5 ultimately find the next nearest neighbor required to anchor a Mo dimer or to dehydrate during the extended treatment in air (96 h at 950 K) required for vapor-phase exchange. The apparent high density of Al site pairs in this sample may reflect the migration of Al centers by exchange with Si atoms above 773 K,[42] a process that stops when thermodynamically stable Al−O−Al or Mo−O−Al bonds form via condensation reactions. The required migration can occur via "hopping" into lattice vacancies or defects, via thermally-induced exchange of Si with Al, or by H_2O-assisted diffusion pathways. When Al atoms reside momentarily near another one (as a next nearest neighbor or across a channel), their OH groups react to form H_2O and an O^{2-} vacancy, or exchange with two $(MoO_2OH)^+$, which can then condense to form a $(Mo_2O_5)^{2+}$ dimer containing a bridging oxygen atom. Either event stabilizes Al−O−Al or Al−O−Mo site pairs slightly detached from framework positions, distorted from tetrahedral symmetry, and invisible by ^{27}Al NMR.

^{27}Al NMR data (Figure 7) confirmed the nature of the exchanged Mo species and the details of the migration and exchange processes. The intensity of the line at 56 ppm, corresponding to tetrahedral Al center in the ZSM5 framework, decreased as the Mo content increased for samples with less than 4 wt % Mo; this decrease in intensity was not compensated by the detection of new or more intense NMR lines. At higher Mo contents, the framework Al line was not detected, but strong lines corresponding to $Al_2(MoO_4)_3$ appear. No NMR lines were detected ($\delta = -416$ and 543 ppm) in vapor-exchanged (4.3 wt %) Mo/H-ZSM5 samples. This shows that vapor exchange creates neither Al_2O_3 nor $Al_2(MoO_4)_3$ in samples with this Mo content. The anchoring of $(Mo_2O_5)^{2+}$ dimers appears to form Mo−O−Al bonds that distort the tetrahedral structure of framework Al centers, leading to the typical broadening of lines for quadrupolar Al nuclei with decreasing symmetry.[43] The Al symmetry at exchange sites bonded to $(Mo_2O_5)^{2+}$ dimers differs markedly from that observed in known Al compounds. Al^{3+} centers have tetrahedral coordination in aluminosilicate frameworks and octahedral symmetry in γ-Al_2O_3. $Al_2(MoO_4)_3$ has

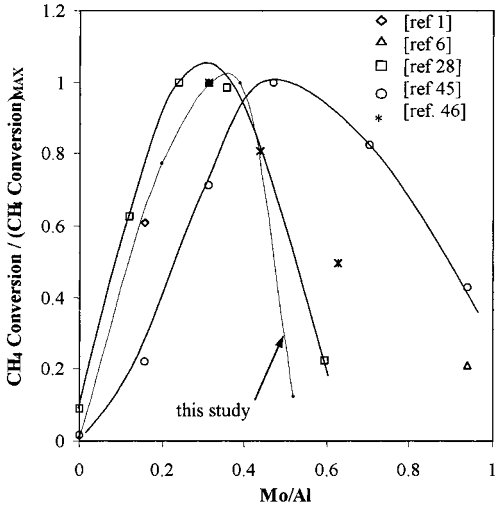

Figure 15. Literature reports of CH_4 conversion, normalized by the maximum conversion reported in each study, as a function of Mo/Al ratio. The solid lines connect data from a single study.

octahedral Al centers and tetrahedral Mo centers, while $(Mo_2O_5)^{2+}$ dimers located at two cation exchange sites would have distorted tetrahedral Al centers bound to distorted tetrahedral Mo^{6+}; it is this required distortion that leads to the broadening of NMR lines after exchange or dehydroxylation of zeolites.

Formation of Active Sites during CH_4 Aromatization. The predominant formation of CO_x, H_2O, and H_2 during initial contact of MoO_x/H-ZSM5 with CH_4 at 950 K (Figure 1) and the increase in hydrocarbon formation rates with increasing time on stream suggest that active sites are created by the reduction and carburization of $(Mo_2O_5)^{2+}$ species that are not active for methane conversion to hydrocarbons. Sites in $(Mo_2O_5)^{2+}$ dimers react with C−H bonds in CH_4, but they cannot desorb the resulting fragments, which form instead MoC_x species via subsequent dehydrogenation steps. Catalytic CH_4 activation begins only after reduced Mo species are passivated by the formation of these carbide species, which are then able to desorb reaction products and complete a turnover. The high melting point and the low volatility of Mo suboxides and carbides[11] suggest that migration is unlikely to occur after reduction−carburization of exchanged $(Mo_2O_5)^{2+}$. These conclusions are consistent with detailed characterization studies reported elsewhere.[44,47]

Exchanged $(Mo_2O_5)^{2+}$ species are precursors to CH_4 activation sites in Mo/H-ZSM5 catalysts. Therefore, CH_4 conversion rates increase with increasing extent of Mo exchange during synthesis. Reaction pathways, however, also require Bronsted acid sites, provided by the remaining H^+ species in ZSM5. These acid sites catalyze chain growth and cyclization reactions of the initial ethylene products formed in CH_4 activation steps; thus, acid sites shift the product distributions toward aromatics, which are favored over alkenes by thermodynamics. As a result, the fraction of the Al sites exchanged by Mo (Mo/Al), and not the Mo content, becomes the relevant parameter determining catalytic rates. Our H-ZSM5 samples (Si/Al = 14.3) lose about 40% of the framework Al sites during air treatment at 973 K; for these samples, the optimum Mo concentration for CH_4 aromatization is about 0.4 Mo/Al (Figure 15) or about 0.7 Mo/Al_F if only framework Al are assumed to stabilize H^+. In these samples, the remaining Bronsted acid sites are sufficient to catalyze C_2H_4 aromatization reactions to near-equilibrium levels. Figure 15 shows our data and those from previous studies,[1,6,28,45,46] as CH_4 reaction rates vs Mo/Al ratio. All studies detect maximum relative rates on catalysts with 0.3−0.5 Mo/Al ratios, even though the zeolite Si/Al ratio varied over a wide range (12.5−50) in these samples.

Conclusion

CH_4 conversion rates on catalysts prepared from mixtures of MoO_3 and H-ZSM5 powders are very similar to those obtained on samples prepared via aqueous impregnation−exchange methods. The simpler synthesis from physical mixtures allows measurements of the kinetics of formation and of the stoichiometry of exchanged MoO_x species. H_2O evolved during heating reflects the kinetics of condensation pathways that anchor MoO_x at zeolite exchange sites. Isotopic equilibration between D_2 and residual OH groups after exchange gives the fraction of H^+ species replaced by exchanged Mo oxo cations. The mechanism of exchange involves the initial formation of an external MoO_3 monolayer on zeolite crystals via surface migration at 623−773 K. When the Mo content exceeds that required to form a monolayer (~4−5 wt % Mo in the H-ZSM5 used), MoO_x species are lost as $(MoO_3)_n$ oligomers via sublimation or as unreducible and inactive $Al_2(MoO_4)_3$ domains via reactions with framework Al atoms. Between 773 and 973 K, surface and gas-phase transport paths lead to migration of MoO_x species into zeolite channels and to reactions with OH groups to form $MoO_2(OH)^+$ species that condense quickly to form H_2O and a strong Mo−O−Al anchoring bond. The amount of H_2O evolved during exchange and the number of H^+ remaining after exchange are consistent with the replacement of one H^+ by each exchanged Mo. This stoichiometry and the requirement for charge neutrality during exchange lead to the proposal that Mo species exist as $(Mo_2O_5)^{2+}$ ditetrahedra interacting with two zeolite exchange sites. These $(Mo_2O_5)^{2+}$ dimers reduce and carburize during methane reactions to form the active MoC_x sites required for catalytic C−H bond activation. Maximum rates are observed on catalysts with intermediate Mo/Al ratios (~0.4), because both exchanged cations and residual Bronsted acid sites are required for the conversion of methane to C_6+ aromatics.

Acknowledgment. R.B. was supported by a National Science Foundation Fellowship. Y.-H.K. was supported by the Korean Science and Engineering Foundation (KOSEF). The project was funded by the Federal Energy Technology Center of the U.S. Department of Energy (DE-AC03-76SF00098) under the technical supervision of Dr. Daniel Driscoll.

References and Notes

(1) Wang, L.; Tao, L.; Xie, M.; Xu, G. *Catal. Lett.* **1993**, *21*, 35.

(2) Solymosi, F.; Erdohelyi, A.; Szoke, A. *Catal. Lett.* **1995**, *32*, 43.

(3) Wang, D.; Lunsford, J. H.; Rosynek, M. P. *Top. Catal.* **1996**, *3*, 289.

(4) Liu, S.; Dong, Q.; Ohnishi, R.; Ichikawa, M. *J. Chem. Soc., Chem. Commun.* **1997**, 1455.

(5) Stakheev, A. Y.; Khodakov, A. Y.; Kustov, L. M.; Kazansky, V. B.; Minachev, Kh. M. *Zeolites* **1992**, *12*, 866.

(6) Xu, Y.; Shu, Y.; Liu, S.; Huang, J.; Guo, X. *Catal. Lett.* **1995**, *35*, 233.

(7) Dong, Y.; Liu, S.; Zhang, Q.; Liu, J.; Yang, K. *Acta Pet. Sin. (Pet. Process. Sect.)* **1992**, *8*, 66.

(8) Xu, Y.; Liu, S.; Wang, L.; Xie, M.; Guo, X. *Catal. Lett.* **1995**, *135*, 135.

(9) Satterfield, C. N. *Heterogeneous Catalysis in Industrial Practice*, 2nd ed.; McGraw-Hill, Inc.: New York, 1991.

(10) Brewer, L. *Molybdenum: Physico-chemical properties of its compounds and alloys*; International Atomic Energy Agency: Vienna, 1980; Vol. 7.

(11) Knacke, O., Kubaschewski, O., Hesselmann, K., Eds. *Thermochemical Properties of Inorganic Substances II*, 2nd ed.,; Springer-Verlag: Berlin, 1991; Vol. 2.

(12) Vahel, A.; Hubener, S.; Eichler, B. *Radiochim. Acta* **1995**, *69*, 233.

(13) Vahel, A.; Hubener, S.; Dressler, R.; Eichler, B.; Turler, A. *Radiochim. Acta* **1997**, *78*, 53.

(14) Minming, H.; Howe, R. F. *J. Catal.* **1987**, *108*, 283.

(15) Liu, W.; Xu, Y.; Wong, S.-T.; Wang, L.; Qiu, J.; Yang, N. *J. Mol. Catal. A* **1997**, *120*, 257.

(16) Biscardi, J. A.; Meitzner, G. D.; Iglesia, E. *J. Catal.* **1998**, *179*, 192.

(17) H-ZSM5 samples (0% Mo) were heated to higher temperatures (973 K) in order to ensure complete isotopic exchange.

(18) The relaxation delay was 1.0 s, the sweep width was 50 kHz, and all chemical shifts were referred to a dilute $Al(NO_3)_3$ solution. A 90°/180° echo pulse sequence was used and data were collected for 0.35 h. Increasing the relaxation delay between acquisitions did not increase the ^{27}Al NMR signal, indicating that 1.0 s was sufficient to allow full relaxation of all Al spin states. In this case, the NMR signal peak area, integrated using Peakfit (Jandel Scientific), is proportional to the number of Al centers represented in that peak.

(19) Kentgens, A. P. M.; Scholle, K. F. M. G. J.; Veeman, W. S. *J. Phys. Chem.* **1983**, *87*, 4357.

(20) Deng, F.; Du, Y.; Ye, C.; Wang, J.; Ding, T.; Li, H. *J. Phys. Chem.* **1995**, *99*, 15208.

(21) Experiments using unheated lines overestimated the amount of carbon deposited on the catalyst because of condensation of naphthalene and heavier products in the gas transfer lines.

(22) HP 6890 gas chromatograph (Hewlett-Packard) equipped with a Carboxen 1000 packed column (3.2 mm × 2 m, Supelco) connected to a thermal conductivity detector and with a HP-1 capillary column (methyl silicone, 0.32 mm × 50 m × 1.05 mm, Hewlett-Packard) connected to a flame ionization detector.

(23) All gases were $>$99.99% purity (from Praxair and Matheson) and were passed through molecular sieve (13X and 5A) traps before use. Flow rates were metered using electronic mass flow controllers (Porter Instruments).

(24) Wolthuizen, J. P.; van den Berg, J. P.; can Hoof, J. H. C. In *Catalysis by Zeolites*, Imelik, B., Ed.; Elsevier Scientific Publishing Co.: Amsterdam, 1980.

(25) The initial concentration of Mo for this sample was 4.0 wt %, but after temperature-programmed treatment in air up to 973 K the sample contained 3.6 wt % Mo (Table 3).

(26) Wang, D.; Lunsford, J. H.; Rosynek, M. P. *J. Catal.* **1997**, *169*, 347.

(27) The initial Mo concentration for this sample was 8 wt %, but after temperature-programmed treatment in air the sample contained 6.3 wt % Mo (Table 3).

(28) Chen, L.; Lin, L.; Xu, Z.; Li, X.; Zhang, T. *J. Catal.* **1995**, *157*, 190.

(29) In principle, the number of D atoms counted during $H_2(g)/O(s)-D$ exchange should equal the number of H atoms detected during $D_2(g)/O(s)-H$ exchange. The latter, however, was larger for all samples containing Mo, because more D_2 was formed during $H_2(g)/O(s)-D$ exchange than H_2 was during the initial $D_2(g)/O(s)-H$ exchange. One explanation for this discrepancy is that the mass fragmentation pattern of the D_2O reduction peak during the first $D_2(g)/O(s)-H$ exchange contains some H_2O.

(30) This value is less than unity because some acid sites were lost during the conversion of NH_4-ZSM5 to H-ZSM5 at 773 K. This sample also lost additional O−H groups during the initial $D_2(g)/O(s)-H$ exchange, because it required heating to 973 K in order to complete the isotopic exchange. The H/Al values from the second $H_2(g)/O(s)-D$ exchange were used for Mo-containing samples in the calculations shown in Table 4, because this led to a more accurate hydrogen atom balance.

(31) Zhang, J.-Z.; Long, M. A.; Howe, R. F. *Catal. Today* **1998**, *44*, 293.

(32) Lunsford, J. H.; Rosynek, M. P.; Wang, D. Presented at the 4th International Natural Gas Symposium, Kruger National Park, South Africa, 1995.

(33) Solymosi, F.; Szoke, A. *Symposium on Heterogeneous Hydrocarbon Oxidation, 211th National Meeting, American Chemical Society* (New Orleans, LA), 1996; p 147.

(34) Mestl, G.; Knözinger, H. *Langmuir* **1998**, *14*, 3964.

(35) Regalbuto, J. R.; Ha, J.-W. *Catal. Lett.* **1994**, *29*, 189.

(36) The fact that MoO_x spreading occurs on external ZSM5 surfaces suggests that the Al content in H-ZSM5 has a high enough surface density of Al sites to form $(MoO_x)_n$ oligomers that bridge Al species on the external surface. Si−O−Mo bonds do not appear to be strong enough to survive air treatment at 950 K, since MoO_3 vapor exchange preparation (Figure 6) results in only 4.3 wt % Mo, which is much less than expected if the external ZSM5 surface area was covered and framework OH groups were exchanged with Mo.

(37) Andersson, G.; Magneli, A. *Acta Chem. Scand.* **1950**, *4*, 793.

(38) MoO_3 may eventually spread into a monolayer, but below 773 K the weak bonds between bilayers are more likely to break than the strong Mo−O−Mo bonds within bilayers.

(39) This Mo content (4 wt %) corresponds to about 19 m^2/g for a MoO_3 bilayer or 38 m^2/g for a monolayer.

(40) Pope, M. T. *Heteropoly and Isopoly Oxometalates*; Inorganic Chemistry Concepts; Jorgensen, C. K., Ed.; Springer-Verlag: Berlin, 1983.

(41) Feng, X. B.; Hall, W. K. *Catal. Lett.* **1997**, *46*, 11.

(42) The Tammann temperature of quartz SiO_2 is 940 K, so mobility of ions in the O−Si−O lattice of ZSM5 should occur between 673 and 973 K.

(43) Engelhardt, G.; Michel, D. *High-resolution solid-state NMR of silicates and zeolites*; Wiley, New York, 1987.

(44) Borry, R. W.; Li, W.; Meitzner, G.; Iglesia, E. *J. Catal.* submitted for publication.

(45) Xu, Y.; Liu, W.; Wong, S.-T.; Wang, L.; Guo, X. *Catal. Lett.* **1996**, *40*, 207.

(46) Pinglian, T.; Zhusheng, X.; Tao, Z.; Laiyuan, C.; Liwu, L. *React. Kinet. Catal. Lett.* **1997**, *61*, 391.

(47) Borry, R. W.; Lu, E. C.; Kim, Y. H.; Iglesia, E. *Stud. Surf. Sci. Catal.* **1998**, *119*, 403.